

INTEGRAL/RossixTE high-energy observation of a state transition of GX 339{4

T. Belloni^{1,2}, I. Parolin¹, M. Del Santo², J. Homann³, P. Casella¹, R. P. Fender⁴,
W. H. G. Lewin³, M. Mendez⁵, J. M. Miller⁶, M. van der Klis⁷

¹INAF-Osservatorio Astronomico di Brera, Via E. Bianchi 46, I-23807 Merate (LC), Italy

²INAF-Istituto di Astrofisica Spaziale e Fisica Cosmica di Roma, Via Fosso del Cavaliere 100, I-00133 Roma, Italy

³Center for Space Research, Massachusetts Institute of Technology, 77 Massachusetts Avenue, Cambridge, MA 02139-4307, USA

⁴School of Physics and Astronomy, University of Southampton, Southampton, Hampshire SO17 1BJ

⁵SRON, Netherlands Institute for Space Research, Sorbonnelaan 2, 3584 CA Utrecht, The Netherlands

⁶Center for Space Research, Massachusetts Institute of Technology, 77 Massachusetts Avenue, Cambridge, MA 02139-4307, USA

⁷Astronomical Institute "Anton Pannekoek", University of Amsterdam, and Center for High Energy Astrophysics, Kruislaan 403, 1098 SJ, Amsterdam, The Netherlands

Accepted 2005 December 29 Received 2005 November 10

ABSTRACT

On 2004 August 15, we observed a fast (shorter than 10 hours) state transition in the bright black-hole transient GX 339{4 simultaneously with RossiXTE and INTEGRAL. This transition was evident both in timing and spectral properties. Combining the data from PCA, HEXTE and IBIS, we obtained good quality broad-band (3–200 keV) energy spectra before and after the transition. These spectra indicate that the hard component steepened. Also, the high-energy cutoff that was present at 70 keV before the transition was not detected after the transition. This is the first time that an accurate determination of the broad-band spectrum across such a transition has been measured on a short time scale. It shows that, although some spectral parameters do not change abruptly through the transition, the high-energy cutoff increases/disappears rather fast. These results constitute a benchmark on which to test theoretical models for the production of the hard component in these systems.

Key words: X-ray: binaries { accretion: accretion discs { black hole: physics

1 INTRODUCTION

Black-hole candidate X-ray binaries (BHCs) are known to show transitions between different spectral states since the first observations of Cyg X-1 (Tananbaum et al. 1971). When X-ray instrumentation became sufficiently sophisticated to allow detailed variability studies on short time scales, the definitions of states were refined to include fast timing properties (van der Klis 1995, 2005; McClintock & Remillard 2005). The number and defining properties of these states have changed with time (see e.g. Homann et al. 2001), but it is now clear that fast variability is key ingredient which needs to be considered in order to have a complete view of the states and state transitions. The spectral evolution of BHCs has recently been described in terms of the pattern in an X-ray hardness-intensity diagram (HID) (see Homann & Belloni 2005; Belloni et al. 2005; Belloni 2005). Original states are found to correspond to different branches/areas

of a q-like HID pattern. Four main states are identified within this framework. Two of them correspond to the original states discovered in the seventies. The Low/Hard State (LS), observed usually at the beginning and at the end of an outburst, and the most common state for the persistent system Cyg X-1 (see e.g. Dove et al. 1998; Pottschmidt et al. 2003; Cadolle Belet al. 2005), is identified by the presence of strong (> 30% fractional rms) band-limited noise in the power spectrum and by a hard energy spectrum. The High/Soft State (HS) shows weak variability, in the form of a few % fractional rms power-law component in the power spectrum, and an energy spectrum dominated by a thermal disc component, with the presence of an additional weak power-law component. The HS is usually observed, if at all, in the central intervals of an outburst; it is the most common state in the persistent systems LMC X-1 and LMC X-3 (Nowak et al. 2001; Wilms et al. 2001; Haardt et al. 2001). For a comparative example of these two states, see Belloni et al. (1999). In between these two well-established states, the situation is rather complex and has led to a number of dif-

² E-mail: belloni@merate.mi.astro.it

ferent classifications. Hornan & Belloni (2005) identify two additional states, clearly defined by spectral/timing transitions. In the evolution of a transient, after the LS comes a transition to the Hard Intermediate State (HIMS): the energy spectrum softens as the combined result of a steepening of the power-law component and the appearance of a thermal disc component. At the same time, the characteristic frequencies in the power spectrum increase and the total fractional rms decreases. A type-C QPO (see Casella, Belloni & Stella 2005) appears, also with centroid frequency increasing as the source softens (see Belloni et al. 2005). The transition to the Soft-Intermediate State is very sharp (sometimes over a few seconds, see Nespoli et al. 2003) and is marked by the disappearance of the type-C QPO and by the appearance of a type-B QPO. In the 3–20 keV range, the corresponding variations in the energy spectrum are rather minor (Belloni et al. 2005). Together with the association of this transition with the ejection of fast relativistic jets, this has led to the identification of a “jet line” in the HID, separating these states (Fender, Belloni & Gallo 2004). The jet line can be crossed more than once during an outburst (as in the case of XTE J1859+226: Casella et al. 2004; Brackston et al. 2002).

While the physical nature of the soft component is commonly associated with an optically thick accretion disc, there is no consensus as to the origin of the hard power-law component, where a power law is probably a simplification of a much more complex reality. The energy spectra include also additional components, important for the physics of accretion around black holes, as emission line features (see e.g. Reynolds & Nowak 2003, Miller et al. 2002, Miller et al. 2004a) and Compton reflection bumps (see e.g. George & Fabian 1991, Zdziarski et al. 2001, Frontera et al. 2001). The spectral slope of the hard component is around 1.6 for the LS, 1.6–2.5 in the SIMS/HIMS and 2.5–4 for the HS. One important parameter to measure is the presence/absence of a high-energy cutoff in the spectrum, for which observations at energies > 20 keV are necessary. It is known since a long time (Sunyaev & Tiumper 1979) that the LS spectrum does show such a cutoff around 100 keV. A comparative measurement of a number of systems with CGRO/OSS has been presented by Grove et al. (1998). Here the energy spectra can clearly be divided into two classes: the ones with a strong soft thermal component and no evidence of a high-energy cutoff until 1 MeV, and those with no soft component and a 100 keV cutoff. While the second class can clearly be identified with the LS, an identification of the first class is not clear. Since both the SIMS/HIMS and the HS show a strong soft component (see e.g. Nespoli et al. 2003) and OSS integration times are very long, different states could be mixed, making a precise identification of the source state uncertain. More recently, Zdziarski et al. (2001) and Rodriguez et al. (2004) measured the high-energy spectrum of GRS 1915+105 and found no direct evidence for a high-energy cutoff, but spectra which appeared to contain two components. A hybrid model was found to be necessary to interpret the spectra of Cyg X-1 (Malzac et al. 2005; Cadolle Belet et al. 2005).

The nature of the hard component in BHCs is not known, nor is it known whether the ones observed in the HS and the LS have the same physical origin. For the LS, different models include thermal componentization (e.g. Dove

et al. 1997, 1998), bulk motion Comptonization (e.g. Laurent & Titarchuk 1999), jet synchrotron plus Comptonization (e.g. Marko, Falcke & Fender 2001; Marko, Nowak & Wills 2005). For the HS, the situation is less clear, partly because of the limited statistics available in the soft spectra and partly because of the absence of an observed characteristic energy such as a high-energy cutoff. Possible models involve non-thermal/hybrid Comptonization (e.g. Gierlinski et al. 1999; Zdziarski et al. 2001; Malzac et al. 2005; Cadolle Belet et al. 2005) and bulk-motion Comptonization (e.g. Turolla, Zane & Titarchuk 2002).

GX 339(4) was one of the first two BHCs for which a complete set of transitions has been observed and studied (see Miyamoto et al. 1991; Belloni et al. 1997; Mendez & van der Klis 1997). This transient black-hole candidate is known to spend long periods in outburst. Historically, it was found prevalently in a hard state, although several transitions were reported (Maejima et al. 1984; Ilovaisky et al. 1986; Miyamoto et al. 1991). From the launch of the Rossi X-Ray Timing Explorer (RXTE) until 1999 it remained detectable with the RXTE All-Sky Monitor, mostly in the Low/Hard state but with a transition to a softer state in 1998 (see Nowak, Wills & Dove 1999; Wills et al. 1999; Belloni et al. 1999; Nowak, Wills & Dove 2002; Corongiu et al. 2003). In 1999, the source went into quiescence, where it was detected with Chandra BeppoSAX at low flux levels (Kong et al. 2000; Corbel et al. 2003).

After roughly one year in quiescence, a new outburst started in 2002 (Smith et al. 2002a,b; Nespoli et al. 2003; Belloni 2004; Hornan et al. 2005) and ended in 2003 (Buxton & Bailyn 2004a). This new outburst was followed in detail through timing and color analysis (Belloni et al. 2005), which made it the prototype for the HID evolution and the definitions of the HIMS/SIMS. In particular, a very clear HIMS-SIMS transition was observed on 2003 May 17, with fast changes in the variability properties, but almost no variations in the 3–20 keV energy spectrum (Hornan et al. 2005). A relativistically broadened iron emission line has been detected in the X-ray spectrum of GX 339(4), indicating the presence of a non-zero angular momentum in the black hole (Miller et al. 2004a,b). A comparative spectral analysis of all existing RXTE data from GX 339(4) is presented by Zdziarski et al. (2004).

GX 339(4) was also the first BHC showing radio/X-ray and near-IR/X-ray correlations in the LS (Hannikainen et al. 1998; Corbel et al. 2003; Marko et al. 2003; Hornan et al. 2005). Radio observations during the 1999 HS showed clear evidence of a strong decrease of core radio emission during this state (Fender et al. 1999). During the 2002/2003, near to the transition to the VHS (see Smith et al. 2002c), a bright radio flare was observed (Fender et al. 2002), which led to the formation of a large-scale relativistic jet (Gallo et al. 2004). Fender, Belloni & Gallo (2004) associated this flare and subsequent ejections with the crossing of the jet line, i.e. the HIMS-SIMS transition reported by Nespoli et al. (2003).

A high mass function ($5.8 \pm 0.5 M_{\odot}$) has been measured for the system (Hynes et al. 2003), indicating strong dynamical evidence for the black-hole nature of the compact object. The distance to GX 339(4) is not well known, with a lower limit of ~ 6 kpc (Hynes et al. 2004; see also Zdziarski et al. 1998).

It is clear that GX 339{4 is an extremely important source for our understanding of the accretion and ejection properties of stellar-mass black holes. In February 2004, after having returned to quiescence, GX 339{4 started a new outburst (Buxton et al. 2004, Smith et al. 2004, Belloni et al. 2004, Kuulkers et al. 2004, Israel et al. 2004).

2 OBSERVATIONS

In August 2004, X-ray and infrared observations of GX 339{4, compared to the previous 2002/2003 outburst, indicated that the source had entered the HIMS and was softening (Buxton & Bailyn 2004b, Homan 2004). This suggested an oncoming transition to the SIMS (see Smith & Bushart 2004) and prompted us to trigger our RXTE/INTEGRAL campaign. Both RXTE and INTEGRAL observed the source on 2004 August 14-16. We report here the results of the joint analysis of RXTE/PCA, RXTE/HEXTE and INTEGRAL/IBIS data.

2.1 RossiXTE

Throughout our campaign, RXTE observed GX 339{4 for seven satellite orbits. We also analyzed four observations from the RossiXTE public archive, two were done before and the two after our observations. In addition, we extracted background-subtracted PCU2 count rates from a number of public observations in the time interval MJD 53195-53240. The log of the observations is shown in Tab.1. We extracted PCA and HEXTE background-corrected energy spectra from each of the intervals in Tab.1 using the standard RXTE software contained in the package HEASOFT 6.0, following the standard procedures. For HEXTE, we limited our analysis to cluster A. To account for residual uncertainties in the calibration, we added a systematic error of 0.6% to the PCA spectra. When necessary (see below), we added spectra using the standard tool `mathpha`. For the production of the outburst light curve and the corresponding H₀, we accumulated background corrected PCU2 rates in the channelbands A = 6-48 (2.5-20.2 keV), B = 6-14 (2.5-6.1 keV) and C = 23-44 (9.4-18.5 keV), defining the hardness as $H = C/B$ (see Homan & Belloni 2005). For the timing analysis of the PCA data, for each of the observation intervals we produced power spectra from 16s stretches accumulated in two channelbands: 0-35 (2-15 keV) and 36-96 (15-40 keV) with a time resolution of 1/128 and 1/2048 seconds. This resulted in eleven spectrograms for each energy band (see Nespoli et al. 2003). The power spectra were normalised according to Leahy et al. (1983) and converted to squared fractional rms (Belloni & Hasinger 1990). For different time selections (see below), we averaged the power spectra and contribution due to Poissonian statistics (see Zhang et al. 1995). The timing analysis was performed with custom software.

2.2 INTEGRAL

As part of the open time program (AO2), INTEGRAL (Winkler et al. 2003) observed GX 339{4 from Aug 14 21:14 UT to Aug 16 05:29 UT. This 102 ks observation was performed with a 5x5 dither pattern for a total of 47 pointings, namely

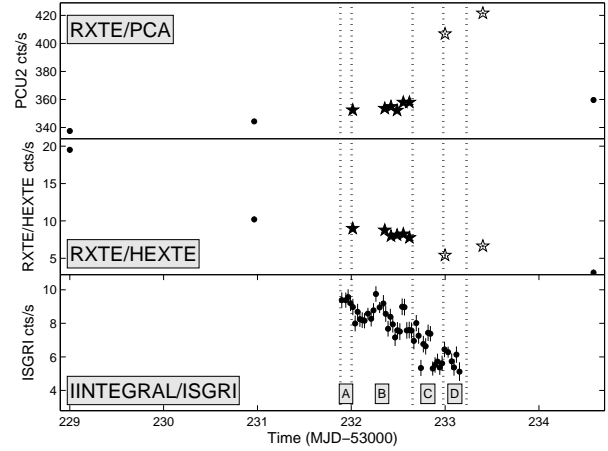


Figure 1. RossiXTE and INTEGRAL light curves of GX 339{4 during our campaign, plus two RossiXTE observations before and two after our points. The energy ranges are 2.9-20.6 keV (PCA), 20-40 keV (HEXTE and ISGRI). The dotted lines separate the four spectral intervals used for spectral analysis (see text). Filled stars mark the observation overlapping with INTEGRAL before the transition. Empty stars indicates the points corresponding to Obs. # 9 and # 10.

"science windows" (SCW), ranging in duration from 1967 s to 4476 s. In each SCW the target is located in a different part of the instruments' field of view. Thanks to the large IBIS' field of view (Ubertini et al. 2003), GX 339{4 was always in its fully coded field of view (9° × 9°) where the nominal sensitivity of coded mask instruments remains constant. On the contrary, due to the smaller field of view and the dithering strategy, the JEM-X coverage of the sky is considerably smaller (Lund et al. 2003).

In this paper we concentrate on the analysis of data collected with ISGRI (Lebrun et al. 2003), the low energy detector layer of IBIS. The IBIS/ISGRI scientific analysis has been performed using the `ibis.science.analysis` main script, included in the latest release of the INTEGRAL online analysis software, OSA 5.0. The ISGRI light curves with a binning time of the SCW duration were obtained extracting the count rate from images. The spectra have been extracted SCW by SCW with the `ii.spectra.extract` script in 16 logarithmic bins spanning from 13 keV to 1 MeV. The response matrices (RMF and ARF) used for spectral fitting have been delivered with OSA 5.0 distribution.

3 RESULTS

In Fig. 1, we plot the light curves of the three instruments (2.9-20.6 keV for PCA, and 20-40 keV for HEXTE and ISGRI). The high-energy curves (HEXTE and ISGRI) show a decrease by a factor of two between MJD 53229 and 53231, followed by another drop by a factor of two during the MJD 53232 observations. After a small recovery, the HEXTE flux drops further. In the PCA band, however, the evolution is different. After a moderate increase until MJD 53232 (Obs. # 8), a much faster brightening is observed at the begin-

Obs.	Type	Start (UT)	End (UT)	Exp. (s)
# 1	P	Aug 11 23:47	Aug 12 00:05	1080
# 2	P	Aug 13 23:01	Aug 13 23:17	960
# 3	C	Aug 15 00:11	Aug 15 00:33	1270
# 4	C	Aug 15 08:05	Aug 15 09:03	3460
# 5	C	Aug 15 09:41	Aug 15 10:38	3420
# 6	C	Aug 15 11:14	Aug 15 12:12	3480
# 7	C	Aug 15 12:49	Aug 15 13:47	3480
# 8	C	Aug 15 14:23	Aug 15 15:21	3480
# 9	C	Aug 15 23:49	Aug 16 00:09	1170
# 10	P	Aug 16 09:21	Aug 16 10:14	3180
# 11	P	Aug 17 13:58	Aug 17 14:13	900

Table 1. Log of the RossiXTE observations analyzed in this work. ‘C’ indicates observations from our campaign, ‘P’ observations from the public archive. 2004 August 11 00:00 UT corresponds to MJD 53228.

ning of MJD 53233 (Obs. # 9), by a factor of 15%. Notice that the sparseness of the PCA points does not allow us to follow the evolution between Obs. # 8 and Obs. # 9. The observed evolution suggests that a transition took place between them.

In order to understand our observations in terms of the global evolution of the outburst, we accumulated from the public RossiXTE archive a light curve and a H/D with the parameters described in the previous section, chosen to be compatible with the definitions used by Homann & Belloni (2005). They can be seen in Fig. 2. Notice that the currently available public data only cover part of the outburst and for this reason the left and bottom branches for this outburst are missing. It is evident from Fig. 2 that the evolution is very similar to that of the previous 2002/2003 outburst (see also Belloni et al. 2005): a monotonic increase of count rate at a rather high color (corresponding to the LS), a horizontal branch with the source softening at a nearly constant count rate (the HIMS), further softening with a transition to the SIMS (see below), and further observations at very low hardness, corresponding to the HS. Notice how the change in hardness between Obs. # 3-8 and Obs. # 9 is rather large and takes place on a time scale of a few hours. However, a striking difference between this outburst and the previous ones is the count rate level of the horizontal/transitional branch, which here is a factor of 3.5 lower.

3.1 Timing analysis

We examined the high-energy power spectra searching for high-frequency features, but none were found. In the following, by power spectra we mean the low-energy (2-15 keV) power spectra. Examining the power spectra, the presence of a transition becomes evident. The power spectrum of Obs. # 1 shows strong band-limited noise, which we fitted with the sum of two zero-centered Lorentzian components (see Belloni, Paltis & van der Klis 2002). The integrated 0.1-64 Hz fractional rms is 23.8%. The power spectra of Obs. # 2 through # 8 are characterised by an integrated 0.1-64 Hz fractional rms decreasing from 18.7 to 15.3% (see top panel of Fig. 3) and complex shape. We fitted it with a combination of six Lorentzian components. The power spectrum of Obs. # 8, together with the best-fit Lorentzian models,

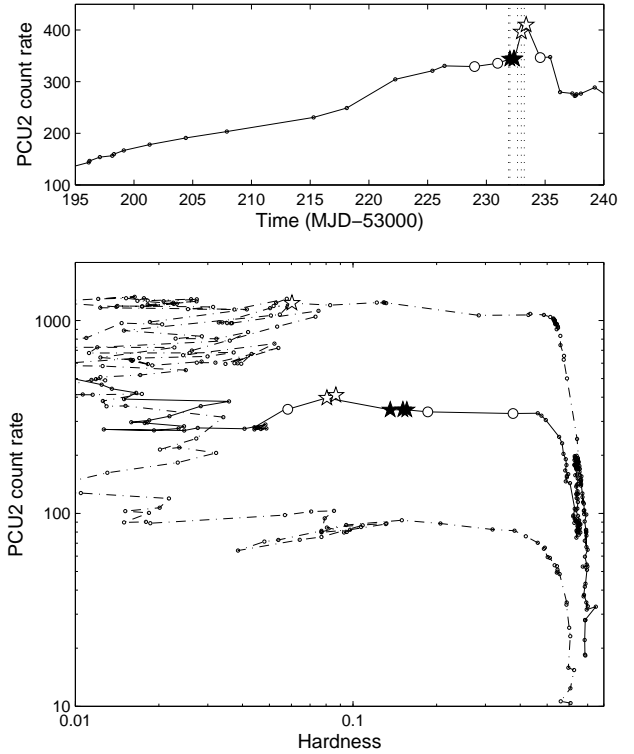


Figure 2. Top panel: PCU2 2.9-20.6 keV net light curve of GX 339+4 from the public RossiXTE archive until a few days after the observations described here. The symbols follow the same convention as in Fig. 1. Bottom panel: Hardness-Intensity diagram from the 2004 outburst (continuous line, outburst not complete here) and from the 2002/2003 outburst (dot-dashed line). The time sequence for both curves starts at the bottom right. For the 2002/2003 curve, the empty star marks the first SIMS point (Nespoli et al. 2003; Belloni et al. 2005).

can be seen in Fig. 4. The sharp QPO peak visible at 6 Hz, appearing together with the band-limited noise component at 1 Hz, can be identified with the type-C QPO (called L_q in Belloni et al. 2002, see Casella et al. 2005) and the corresponding low-frequency component L_b , with characteristic frequencies (see Belloni et al. 2002 for a definition) separated by a factor of 5 (see Wijands & van der Klis 1999). The L_b component requires a second narrower Lorentzian for a good fit. The narrow QPO, as usual, shows a second harmonic peak at twice its frequency (its best-fit frequency was consistent with twice that of the L_q component and was therefore fixed to twice that value), and on its high-frequency flank shows an additional component (L_h in Belloni et al. 2002). There is however a sixth component, with a characteristic frequency of 4 Hz, which cannot be obviously identified (marked with a thick line in Fig. 4). Its frequency is not consistent with being half that of the high-frequency flank described above, indicating that these two components are not harmonically related. The evolution of the centroid frequency of the type-C QPO and of this additional component are shown in the bottom panel of Fig. 3:

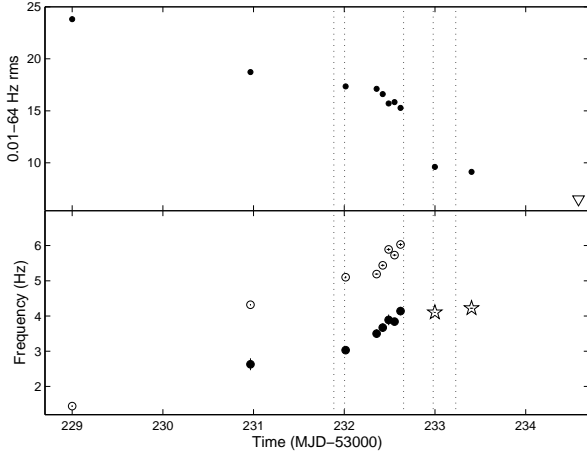


Figure 3. Time evolution of selected timing parameters. Top panel: integrated 0.1-64 Hz fractional rms. Bottom panel: characteristic frequency of the type-C QPO (open circles), of the 4 Hz broad component in Obs. # 3-# 8 (filled circle, see Fig. 4), and of the type-B QPO in Obs. # 9 (stars). The inverted triangle represents a 3-sigma upper limit, error bars are 1-sigma. The vertical dotted lines correspond to those in Fig. 1.

both of them increase with time, when at the same time the source softens (see Fig. 1), which is a behaviour observed in all black-hole transients in the HIMS. Indeed, the shape of the power spectrum, with strong band-limited noise and a type-C QPO, indicate that GX 339{4 was in the HIMS during the first part of the campaign (Obs. # 2 through # 8), after one observation (# 1) which did not show a significant QPO and could be classified as LS. Notice from Fig. 3 (bottom panel) that the frequency of the C-type QPO increases with time until reaching a value of 6 Hz, which appears to be a critical value for type-B QPOs (see Casella, Belloni & Stella 2005). It is not clear whether this value is a coincidence, as in other systems the C-type QPO frequency just before the transition is higher (see e.g. Casella et al. 2004).

The power spectrum of Obs. # 9, about nine hours after # 8, appears completely different (see bottom panel in Fig. 4). The noise level is much lower and can be fitted with one single low-frequency weak Lorentzian, and only one strong QPO component at 4.10 Hz is present, with an additional first harmonic peak (which once again was fixed for the fits to have a centroid frequency twice that of the fundamental). The integrated fractional rms drops to less than 10% (see Fig. 3). The peak can be identified with a type-B QPO (see Wijnands, Homan & van der Klis 1999; Remillard et al. 2002; Casella et al. 2005) and this power spectrum, together with the marked softening visible in Fig. 1 clearly indicates that the source has entered the SIMS (Belloni et al. 2005; Homan & Belloni 2005; Belloni 2005). Notice that the centroid of the type-B QPO (4.10 ± 0.01 Hz) is compatible with the characteristic frequency of the additional component in the power spectrum from Obs. # 8 (4.14 ± 0.12 Hz, 1-sigma errors), suggesting a possible identification of the latter. Obs. # 10 shows a very similar power spectrum. The power spectrum of Obs. # 11 shows no significant noise, with a 3-sigma upper limit

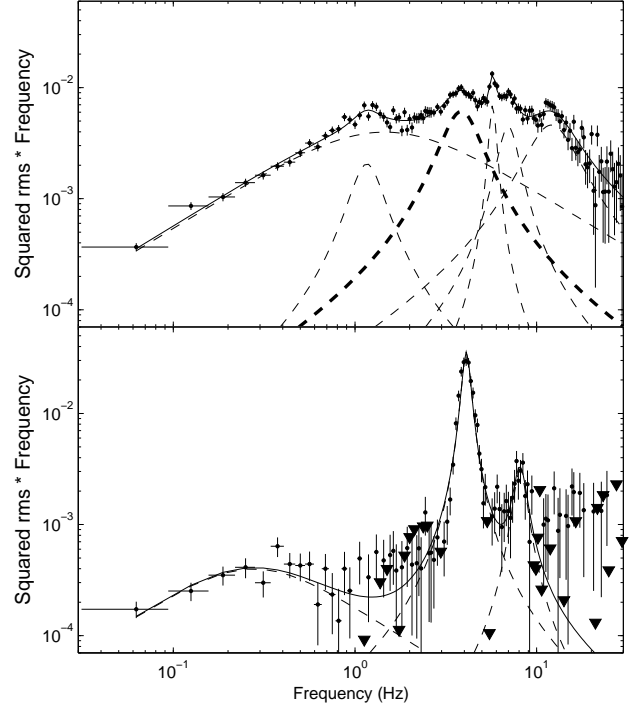


Figure 4. Power spectra from PCA data (2-15 keV) of Obs. # 8 (top) and # 9 (bottom), in P representation. The dashed lines indicate the best-fit Lorentzian components. The thick dashed line in the upper panel shows the component with a frequency similar to that of the main QPO peak in the bottom panel. The scales of the two panels are the same. The triangles correspond to 3-sigma upper limits.

of 6.5% to the 0.1-64 Hz fractional rms, suggesting that the source entered the HS.

3.2 Spectral analysis

Given the sparseness of the # 3-# 9 RXTE observations and the evolution of the flux in the three instruments, we divided the data into four intervals, whose time limits are shown in Tab. 2. The intervals were defined in this way: from the start of the INTEGRAL data until Obs. # 3 (interval A), covering Obs. # 3-# 8 (B), between Obs. # 8 and # 9 (C), and from Obs. # 9 to the end of the INTEGRAL data (D). With this definition, intervals B and D contained both RossiXTE and INTEGRAL data, while intervals A and C were only covered by INTEGRAL. We included Obs. # 3 in interval B because including it in interval A resulted in a best-fit completely compatible with that for interval B. Therefore, we decided for this subdivision which maximizes the statistics for interval B. In order to obtain a good broadband spectrum of GX 339{4, we had to limit our analysis to intervals B (corresponding to the HIMS) and D (SIMS). The remaining intervals were covered, although sparsely, by the JEM-X1 instrument on board INTEGRAL. However, to date it was not possible to extract good spectra from that

Interval	Start (UT)	End (UT)
A	Aug 14 21:14	Aug 15 00:04
B	Aug 15 00:05	Aug 15 15:40
C	Aug 15 15:42	Aug 15 23:30
D	Aug 15 23:32	Aug 16 05:29

Table 2. The four time intervals used for spectral extraction of both RossiXTE and INTEGRAL data. 2004 August 11 00:00 UT corresponds to MJD 53228.

instrument, and the light curve from the full observation was not compatible with the PCA one, after restriction to the same energy band. Therefore, in this work we limit our analysis to PCA + HEXTE + ISGRI. For the spectral fits, we used the XSPEC package version 11.2.31.

We fitted the two spectra (interval B and D) with a simple model consisting of a disc-blackbody, a power law and an emission line fixed at 6.4 keV, all modified by interstellar absorption. Since the estimated absorption for GX 339(4 is rather low and we did not have low-energy coverage, we fixed it to $5 \times 10^{21} \text{ cm}^2$ (Mendez & van der Klis 1997; Kong et al. 2000). In order to account for remaining cross-calibration problems, we included multiplicative constants for the HEXTE and ISGRI spectra with respect to the PCA. The best fit values we obtained were 0.9 and 1.1 respectively. The fits with this model gave different results for the two spectra. The spectrum of interval D was fitted well by this model, with a reduced χ^2 of 1.10 for 85 degrees of freedom (see top panel of Fig. 5 and Table 3). For interval B, no satisfactory fit could be obtained, with a minimum reduced χ^2 of 3.65 for 85 degrees of freedom. The residuals suggested the inclusion of a high-energy cutoff (see Fig. 6). With this addition, the reduced χ^2 became 1.07 (for 84 degrees of freedom), a clear improvement, with a best-fit high-energy cutoff of $72^{+10}_{-6} \text{ keV}$. The best-fit parameters are shown in Tab 3. The main spectral changes were: slight softening of the disc-blackbody component, with increased estimated inner radius by a factor of 1.6 \pm 0.3, steepening of the power-law component, and disappearance of the 70 keV high-energy cutoff. In order to set an upper limit to the energy of a possible high-energy cutoff also in the spectrum from interval D, we added such a cutoff and determined the lower limit to its best fit value. We obtained a 90% lower limit of 84 keV. Notice that, although our model of a simple cutoff power law fits the data of interval B satisfactorily, the presence of an additional Compton refection component with a variable refection fraction might qualitatively yield the same effect observed here. However, such a complication to the model is not required by our data. The equivalent width of the 6.4 keV line is 660 eV and 570 eV for interval B and D respectively. Unlike in the case of the sharp transition of 1E 1740.7(2942 observed in May 2001 (Smith, Heindl & Swank 2002), the photon fluxes show variations roughly consistent with those of the energy flux.

4 DISCUSSION

From our results, it is clear that we observed a transition from the HIMS to the SIMS in GX 339(4 on 2004 August 15. The power spectra before and after the transition show

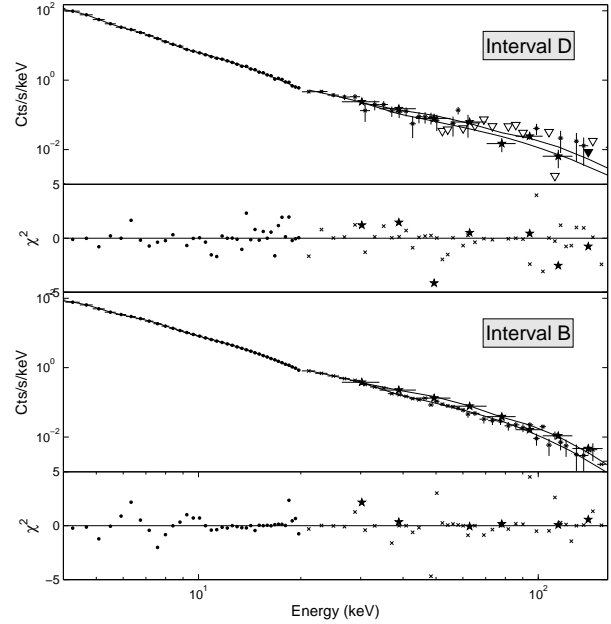


Figure 5. Spectra (PCA: filled circles, HEXTE: crosses; ISGRI: stars) from intervals B and D, with best fit model and residuals.

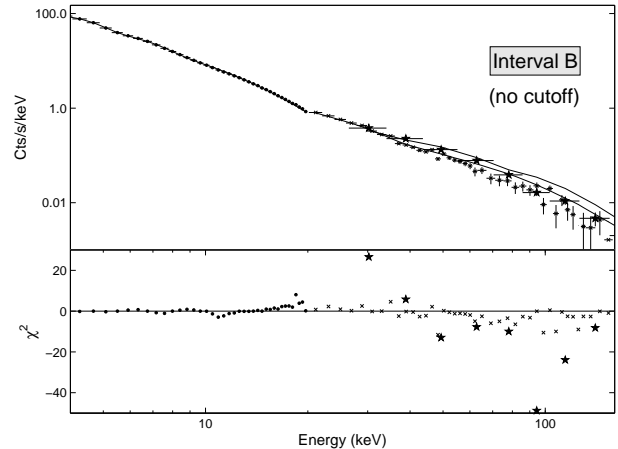


Figure 6. Spectra (PCA: filled circles, HEXTE: crosses; ISGRI: stars) from interval B fitted with a power law without a high-energy cutoff (with best fit model and residuals). The presence of large residuals at high energies is evident.

marked differences: from strong band-limited noise and type-C QPO to much weaker noise and type-B QPO. Thanks to the INTEGRAL coverage of more than one consecutive day, and the simultaneous but more sparse RossiXTE data, we could for the first time follow the transition at high energies and examine in detail the broad-band spectrum before and after the transition. As usual, the transition took place along a nearly horizontal branch in the HID, although at a

different (harder) color position than in 2002 (see Belloni et al. 2005 and Fig. 2).

These changes in timing properties were also observed in the same source during the previous outburst in 2002 (Nespoli et al. 2003; Belloni et al. 2005) and is seen in many black-hole transients (Homan & Belloni 2005; Belloni 2005). Comparing the properties of this transition and those of the analogous transition in the 2002/2003 outburst, we can see that, although the shape of the H₁D is extremely similar (see Belloni et al. 2005; Homan & Belloni 2005), the count rate level of the upper branch is lower by a factor of ~ 3.5 (see Fig. 2). Also, the color at which the transition takes place is not the same: in 2002 it was in the range 0.06–0.08 (notice that the color definition of Belloni et al. 2005 is different than the one adopted here: the colors reported here have been thus re-calculated), while in our data it's between 0.08 and 0.14 (see Fig. 2). This is reflected by the spectral parameters (see below). The fact that the H₁M S branch, while very similar, is substantially lower than in 2002 indicates once more that the transition is not driven by accretion rate only, but another parameter must be at play in causing it. Overall, the evolution through the H₁D follows similar patterns as all other bright transients observed by Rossi XTE, which underwent state transitions (see Homan & Belloni 2005; Belloni 2005).

The evolution of the power spectra is very similar to that of the previous outburst, but here we have the advantage of having a good number of Rossi XTE observations in intervals just before the transition, so that it was possible to follow the evolution of the timing components. What we found is that, as expected, the multiple components in the power spectrum increase their characteristic frequencies. All these features can be identified with known components (Belloni et al. 2002), with the exception of a broad bump around a few Hz (see Fig. 4). The characteristic frequency of this component increases steadily until it reaches a frequency compatible with that of the type-B QPO that appears after the transition (see Fig. 3). It is therefore possible to speculate that these components are related, although we would need more observations of such transitions to assess this identification.

The comparison of the light curves at low and high energies (see Fig. 1) shows that at high energies (> 20 keV), where the hard spectral component dominates, the transition is smooth and takes place over a longer time scale than at low energies. The HEXTE light curve shows that a considerable reduction in flux (a factor of ~ 2) took place in a few days before the transition, and the ISGRI data show a smooth decrease by the same factor within one day across the transition. In other words, the high-energy curves do not allow to locate the transition. On the other hand the transition is much more abrupt at low energies (see the hardness changes in Fig. 2 and the timing changes). Although we do not have complete information on the transition at low energies, due to the limited coverage, we know from other systems that the switch between type-C and type-B QPOs can take place over a few seconds (see e.g. Casella et al. 2004). The fact that spectral transitions are slower than timing transitions was already reported by Kalemci et al. (2004) and can also be seen in the color/timing evolution of GX 339-4 in its previous outburst (Nespoli et al. 2003, Belloni et al. 2005).

Particularly important are the joint Rossi XTE/INTEGRAL spectral fits. The amount of information on the high-energy part of the spectrum in different states of black-hole transients is patchy. In the LS, the broad-band spectrum is well studied, both with simple phenomenological models and with complex detailed physical models (see e.g. Frontera et al. 2001, Zdziarski et al. 2001, Merloni & Fabian 2002, Turolla, Zane & Titarchuk 2002, Malzac, Merloni & Fabian 2004, Falcke, Kording & Marko 2004).

The main features of the LS spectra are a rather flat photon index (~ 1.6) and the clear presence of a high-energy cutoff around 100 keV. The high-energy spectrum of the HS is less well known, due to its softness. Observations with OSSE showed that in states different than the LS, there is no evidence of a high-energy cutoff up to 1 MeV (Grove et al. 1998). However, the integration times needed to accumulate statistically significant OSSE spectra are of the order of weeks, and these observations also cover other states such as the H₁M S and the SIM S, where the hard component is stronger and flatter. Therefore, it is difficult to assess the shape of the high-energy spectra of these states, as transitions can take place on short time scales. Our results constitute one of the first bona-fide broad-band spectral determination of the H₁M S and the SIM S on such a short time scale. The disappearance of the high-energy cutoff in the HEXTE energy band after the transition to the SIM S was already reported for XTE J1650-500, albeit on a slightly longer time scale (Rossi et al. 2005). The H₁M S, which can be considered as an extension of the LS, shortly before the transition to the SIM S, shows a spectral slope of ~ 1.9 and a high-energy cutoff around 70 keV. The spectrum is therefore steeper than in the LS and the high-energy cutoff is at lower energies. After the transition, in the SIM S, the power-law is considerably steeper (~ 2.3), although slightly less than was observed in the previous outburst (~ 2.44 , Nespoli et al. 2003), and there is no evidence of a high-energy cutoff, with a 90% lower limit of 84 keV (in 2002 there was some evidence of a cutoff at 100–200 keV (Nespoli et al. 2003)). Although we cannot exclude the presence of a cutoff, our results show that the cutoff measured in the H₁M S either increases significantly in energy after the transition, or disappears. As to the 4–200 keV luminosity of the system, adopting a distance of 6 kpc (see Hynes et al. 2004), the H₁M S has a luminosity of $2.3 \pm 1.5 \times 10^{36}$ erg/s (disc) and $1.1 \pm 0.2 \times 10^{37}$ erg/s (powerlaw), while in the SIM S the disc flux becomes $3.0 \pm 1.2 \times 10^{36}$ erg/s and the power law flux $9.0 \pm 1.1 \times 10^{36}$ erg/s. The errors due to the flux reconstruction are still rather large and at 90% confidence the disc and power-law luminosities before and after the transition are consistent. These total disc + power law luminosity are therefore around 1–2% of the Eddington luminosity (for 6M \odot). Notice that these values are considerably lower than those in Nespoli et al. (2003) for the 2002 transition, as suggested by the difference in detected count rate. Also, here the power-law component dominates the flux, while in 2002 it did not: this is also reflected by the difference in hardness at the transition. In comparison to what was observed in 2002 (Gallo et al. 2004; Fender, Belloni & Gallo 2004), we would have expected a radio flare to be triggered by the transition (Homan 2004), but unfortunately we could not obtain radio coverage.

Int.	D isc blackbody							(C uto \rightarrow) power law					
	kT [keV]		R _{in} [km]		F _d [erg cm ⁻² s ⁻¹]			E _c [keV]		F _p [erg cm ⁻² s ⁻¹]			
B	0.90	0.05	13	2	5.7	3.8	10 ⁻¹⁰	1.92	0.05	72 ⁺¹⁰ ₋₆	2.7	0.5	10 ⁻⁹
D	0.81	0.03	21	3	7.4	3.0	10 ⁻¹⁰	2.31	0.07		2.2	0.5	10 ⁻⁹

Table 3. Best fit spectral parameters for intervals B and D. For R_{in}, the assumed distance and inclination are 6 kpc and 15° (see Wu et al. 2001). The fluxes are unabsorbed in the 4–200 keV band. Errors represent 90% confidence limits.

5 CONCLUSIONS

The results presented above constitute one of the first determination of the changes of the broad-band X-ray spectrum of a BHC across the HIMS-SIMS transition, which is crucial for the development and testing of theoretical models. Although the transition from the LS to the HS is a process that takes days to weeks (see e.g. Belloni et al. 2005), a sharp transition in the properties of fast time variability takes place on a much shorter time scales. We showed that this transition corresponds also to a change in the high-energy properties.

ACKNOWLEDGMENTS

We thank M. Falanga, A. Bazzano, A. Paizis and I. Kreykenbohm for help in the INTEGRAL analysis. This work was partially supported by ASI grants I/R/046/0, I/R/389/02 and I/R/041/02.

REFERENCES

- Belloni, T., 2004, in *The Restless High-Energy Universe*, E. P. J. van den Heuvel, R. A. M. J. Wijers, J. M. M. in 't Zand Eds., p337
- Belloni, T., 2005, in *Proc. of COSPAR Colloquium \Spectra and Timing of Compact X-Ray Binaries*, Mumbai, India, in press (astro-ph/0507556)
- Belloni, T., Hasinger, G., 1990, *A & A*, 230, 103
- Belloni, T., Psaltis, D., van der Klis, M., 2002, *ApJ*, 572, 392
- Belloni, T., van der Klis, M., Lewin, W. H. G., van Paradijs, J., Dotani, T., Mitsuda, K., Miyamoto, S., 1997, *A & A*, 322, 857
- Belloni, T., Mendez, M., van der Klis, M., Lewin, W. H. G., Dieters, S., 1999, *ApJ*, 519, L159
- Belloni, T., Homann, J., Cui, W., Swank, J., 2004, *ATel*, 236
- Belloni, T., Homann, J., Casella, P., van der Klis, M., Nespoli, E., Lewin, W. H. G., Miller, J. M., Mendez, M., 2005, *A & A*, 440, 207
- Brocksopp, C., Fender, R. P., McCollough, M., Pooley, G. G., Rupen, M. P., Hellmuth, R. M., de la Force, C. J., et al., 2002, *MNRAS*, 331, 765
- Buxton, M., Bailyn, C., 2004a, *ATel*, 270
- Buxton, M., Bailyn, C., 2004b, *ATel*, 316
- Buxton, M., Gallo, E., Fender, R. P., Bailyn, C., 2004, *ATel*, 230
- Cadotte Bel, M., Sizun, P., Goldwurm, A., Rodriguez, J., Laurent, P., Zdziarski, A. A., Foschini, L., et al., 2005, *A & A*, in press (astro-ph/0509851)
- Casella, P., Belloni, T., Homann, J., Stella, L., 2004, *ApJ*, 426, 587
- Casella, P., Belloni, T., Stella, L., 2005, *ApJ*, 629, 403
- Corbel, S., Nowak, M. A., Fender, R. P., Tzioumis, A. K., Marko, S., 2003, *A & A*, 400, 1007
- Corongiu, A., Chiappetti, L., Haardt, F., Treves, A., Coppi, M., Belloni, T., 2003, *A & A*, 408, 347
- Dove, J. B., Wilms, J., Malsack, M., Begelman, M. C., 1997, *ApJ*, 487, 759
- Dove, J. B., Wilms, J., Nowak, M. A., Vaughan, B. A., Begelman, M. C., 1998, *MNRAS*, 298, 729
- Falcke, H., Kording, E., Marko, S., 2004, *A & A*, 414, 895
- Fender, R. P., Belloni, T., Gallo, E., 2004, *MNRAS*, 355, 1105
- Fender, R. P., Corbel, S., Tzioumis, T., McIntyre, V., Campbell-Wilson, D., Nowak, M. A., Sood, R., 1999, *ApJ*, 519, L165
- Fender, R. P., Corbel, S., Tzioumis, T., Tingay, S., Brocksopp, C., Gallo, E., 2002, *ATel*, 107
- Frontera, F., Palazzi, E., Zdziarski, A. A., Haardt, F., Perola, G. C., Chiappetti, L., Cusumano, G., et al., 2001, *ApJ*, 546, 1027
- Gallo, E., Corbel, S., Fender, R. P., Acciarone, T. J., Tzioumis, A. K., 2004, *MNRAS*, 347, L52
- George, I., Fabian, A. C., 1991, *MNRAS*, 249, 352
- Gierlinski, M., Zdziarski, A. A., Poutanen, J., Coppi, P. S., Ebisawa, K., Johnson, W. N., 1999, *MNRAS*, 309, 496
- Grove, J. E., Johnson, W. N., Kroeger, R. A., McNaron-Brown, K., Skibo, J. G., Philips, B. F., 1998, *ApJ*, 500, 899
- Hannikainen, D. C., Hunstead, R. W., Campbell-Wilson, D., Sood, R. K., 1998, *A & A*, 337, 460
- Haardt, F., Galli, M. R., Treves, A., Chiappetti, L., D'Alfiume, D., Corongiu, A., Belloni, T., Frontera, F., Kuulkers, E., Stella, L., 2001, *ApJSuppl*, 133, 187
- Homann, J., 2004, *ATel*, 318
- Homann, J., Belloni, T., 2005, in *From X-ray Binaries to Quasars: Black Hole Accretion on All Mass Scales*, T. J. Acciarone, R. P. Fender, L. C. Ho Eds, Kluwer, Dordrecht, in press (astro-ph/0412597)
- Homann, J., Wijnands, R., van der Klis, M., Belloni, T., van Paradijs, J., Klein-Wolt, M., Fender, R. P., Mendez, M., 2001, *ApJSuppl*, 132, 377
- Homann, J., Buxton, M., Marko, S., Bailyn, C. D., Naspoli, E., Belloni, T., 2005, *ApJ*, 624, 259
- Hynes, R. I., Steeghs, D., Casares, J., Charles, P. A., O'Brien, K., 2003, *ApJ*, 583, L95
- Hynes, R. I., Steeghs, D., Casares, J., Charles, P. A., O'Brien, K., 2004, *ApJ*, 609, 317
- Ilovaisky, S. A., Chevalier, C., Motch, C., Chiappetti, L., 1986, *A & A*, 164, 67
- Israel, G., Covino, S., Kuulkers, E., Zerbini, F. M., Chincarini,

- G., Rodono, M., Antonelli, L. A., 2004, *ATel*, 243
- Kalemci, E., Tom sick, J. A., Rothschild, R. E., Pottschmidt, K., Kaaert, P., 2004, *ApJ*, 603, 231
- Kong, A. K. H., Kuulkers, E., Charles, P. A., Smale, A. P., 2000, *MNRAS*, 311, 405
- Kuulkers, E., Bodaghee, A., Foschini, L., Guainazzi, M., Matt, G., Israel, G., Nicastro, F., et al., 2004, *ATel*, 240
- Laurent, P. Titarchuk, L., 1999, *ApJ*, 511, 289
- Leahy, D. A., Dabro, W., Elsner, R. F., Weisskopf, M. C., Kahn, S., Sutherland, P. G., Gindlay, J. E., 1983, *ApJ*, 266, 160
- Lebrun, F., Leray, J. P., Lavocat, P., Cretolle, J., Arques, M., Blondel, C., Bonnin, C., et al., 2003, *A & A*, 411, L141
- Lund, N., Budtz-Jørgensen, W., Stergaard, N. J., Brandt, S., Rasmussen, I. L., Homstrup, A., Oxborrow, C. A., et al., 2003, *A & A*, 411, L231
- Maejima, Y., Makishima, K., Matsuoka, M., Ogawara, Y., Oda, M., Tawara, Y., Doi, K., 1984, *ApJ*, 285, 712
- Marko, S., Falcke, H., Fender, R. P., 2001, *A & A*, 372, L25
- Marko, S., Nowak, M. A., Wilms, J., 2005, *ApJ*, in press (astro-ph/0509028)
- Malzac, J., Merloni, A., Fabian, A. C., 2004, *MNRAS*, 351, 253
- Malzac, J., Petrucci, P. O., Jourdain, E., Cadolle Bel, M., Sizun, P., Pooley, G., Cabanac, C., et al., 2005, *A & A*, submitted
- Marko, S., Nowak, M. A., Corbel, S., Fender, R. P., Falcke, H., 2003, *A & A*, 397, 645
- McIntock, J. E., Remillard, R. A., 2005, in "Compact stellar X-ray sources", W. H. G. Lewin & M. van der Klis Eds., Cambridge Univ. Press, Cambridge, in press (astro-ph/0306213)
- Mendez, M., van der Klis, M., 1997, *ApJ*, 479, 926
- Merloni, A., Fabian, A. C., 2002, *MNRAS*, 332, 165
- Miller, J. M., Fabian, A. C., Wijnands, R., Remillard, R. A., Woźdowski, P., Schulz, N. S., DiMatteo, T., Marshall, H. L., Canizares, C. R., Pooley, D., Lewin, W. H. G., 2002, *ApJ*, 578, 348
- Miller, J. M., Fabian, A. C., Reynolds, C. S., Nowak, M. A., Homann, J., Freyberg, M. J., Ehle, M., Belloni, T., Wijnands, R., van der Klis, M., Charles, P. A., Lewin, W. H. G., 2004a, *ApJ*, 606, L131
- Miller, J. M., Raymond, J., Fabian, A. C., Homann, J., Nowak, M. A., Wijnands, R., van der Klis, M., et al., 2004b, *ApJ*, 601, 450
- Miyamoto, S., Kitaura, K., Kitamoto, S., Dotani, T., Ebisawa, K., 1991, *ApJ*, 383, 784
- Nespoli, E., Belloni, T., Homann, J., Miller, J. M., Lewin, W. H. G., Mendez, M., van der Klis, M., 2003, *A & A*, 412, 235
- Nowak, M. A., Wilms, J., Dove, J. B., 1999, *ApJ*, 517, 355
- Nowak, M. A., Wilms, J., Dove, J. B., 2002, *MNRAS*, 332, 856
- Nowak, M. A., Wilms, J., Heindl, W. A., Pottschmidt, K., Dove, J. B., Begelman, M. C., 2001, *MNRAS*, 320, 316
- Pottschmidt, K., Wilms, J., Nowak, M. A., Pooley, G. G., Geisner, T., Heindl, W. A., Smith, D. M., 2003, *A & A*, 407, 1039
- Remillard, R. A., Sobczak, G. J., Muno, M. P., McIntock, J. E., 2002, *ApJ*, 564, 962
- Reynolds, C. S., Nowak, M. A., 2003, *PhR*, 377, 389
- Rodríguez, J., Corbel, S., Hannikainen, D. C., Belloni, T., Paizis, A., Vilhu, O., 2004, *ApJ*, 615, 416
- Rossi, S., Homann, J., Miller, J. M., Belloni, T., 2005, *MNRAS*, 360, 763
- Smith, D. M., Bushart, S. K., 2004, *ATel*, 322
- Smith, D. M., Heindl, W. A., Swank, J. H., 2002, *ApJ*, 569, 362
- Smith, D. M., Swank, J. H., Heindl, W. A., Remillard, R. A., 2002a, *ATel*, 85
- Smith, D. M., Belloni, T., Kalemci, E., et al., 2002b, *IAUC*, 7912
- Smith, D. M., Belloni, T., Heindl, W. A., et al., 2002c, *ATel*, 95
- Smith, D. M., Heindl, W. A., Swank, J. H., Wilms, J., Pottschmidt, K., 2004a, *ATel*, 231
- Sunyaev, R. A., Trumper, J., 1979, *Nature*, 279, 506
- Tananbaum, H., Gursky, H., Kellogg, E., Giacconi, A., Jones, C., 1971, *ApJ*, 177, L51
- Turolla, R., Zane, S., Titarchuk, L., 2002, *ApJ*, 576, 349
- Ubertini, P., Lebrun, F., DiCocco, G., Bazzano, A., Bird, A. J., Roenstad, K., Goldwurm, A., et al., 2003, *A & A*, 411, L131
- van der Klis, M., in "X-ray Binaries", W. H. G. Lewin, J. van Paradijs & E. P. H. van den Heuvel Eds., Cambridge Univ. Press, Cambridge, p252
- van der Klis, M., 2005, in "Compact stellar X-ray sources", W. H. G. Lewin & M. van der Klis Eds., Cambridge Univ. Press, Cambridge, in press (astro-ph/0410551)
- Wijnands, R., van der Klis, M., 1999, *ApJ*, 514, 939
- Wijnands, R., Homann, J., van der Klis, M., 1999, *ApJ*, 526, L33
- Wilms, J., Nowak, M. A., Dove, J. B., Fender, R. P., DiMatteo, T., 1999, *ApJ*, 522, 460
- Wilms, J., Nowak, M. A., Pottschmidt, K., Heindl, W. A., Dove, J. B., Begelman, M. C., 2001, *MNRAS*, 320, 327
- Winkler, C., Courvoisier, T. J. L., DiCocco, G., Gehrels, N., Gimenez, A., Grebenev, S., Hemsen, W., et al., 2003, *A & A*, 411, L1
- Wu, K., Soria, R., Hunstead, R. W., Johnston, H. M., 2001, *MNRAS*, 320, 177
- Zdziarski, A. A., Poutanen, J., Mikolajewska, J., Gierlinski, M., Ebisawa, K., Johnson, W. N., 1998, *MNRAS*, 301, 435
- Zdziarski, A. A., Grove, J. E., Poutanen, J., Rao, A. R., Vadawale, V., 2001, *ApJ*, 554, L45
- Zdziarski, A. A., Gierlinski, M., Mikolajewska, J., Wardzinski, G., Smith, D. M., Harmon, B. A., Kitamoto, S., 2004, *MNRAS*, 351, 791
- Zhang, W., Jahoda, K., Swank, J. H., Morgan, E. H., Giles, A. B., 1995, *ApJ*, 449, 930